

# Signature of Chaos and Delocalization in a Periodically Driven Many Body System : An Out-of-Time-Order Correlation Study

S. Ray,<sup>1</sup> S. Sinha,<sup>1</sup> and K. Sengupta<sup>2</sup>

<sup>1</sup>Indian Institute of Science Education and Research, Kolkata, Mohanpur, Nadia 741246, India

<sup>2</sup>Theoretical Physics Department, Indian Association for the Cultivation of Science, Jadavpur, Kolkata-700032, India.

(Dated: April 6, 2018)

We study out-of-time-order correlation (OTOC) for one-dimensional periodically driven hardcore bosons in the presence of Aubry-André (AA) potential and show that both the spectral properties and the saturation values of OTOC in the steady state of these driven systems provide a clear distinction between the localized and delocalized phases of these models. Our results, obtained via exact numerical diagonalization of these boson chains, thus indicate that OTOC can provide a signature of drive induced delocalization even for systems which do not have a well defined semiclassical (and/or large  $N$ ) limit. We demonstrate the presence of such signature by analyzing two different drive protocols for hardcore bosons chains leading to distinct physical phenomena and discuss experiments which can test our theory.

PACS numbers:

*Introduction* : Identifying the signature of chaos in quantum systems is a long standing issue [1, 2] which has relevance for both its entanglement properties [3, 4] and thermalization [5, 6]. Typical fingerprint of chaos in a quantum system may be found in its spectral properties by invoking the BGS conjecture [7]. Recent studies however show that the out-of-time-order correlator (OTOC) provides an alternate and more direct way to quantify chaos even in the interacting many body systems [8–17]. Recent developments in the experimental techniques to measure the quantum correlations enables a direct investigation of the OTOC in trapped ions and spin systems [18, 19]. For quantum systems with a well-defined semiclassical limit, OTOC provides a way to estimate the Lyapunov exponent which may be used to quantify the degree of chaos of the system [8]. Interestingly application of this method in the Sachdev-Ye-Kitaev (SYK) model [20] provides an upper bound to this Lyapunov exponent which is believed to have a connection with the information scrambling in black holes [21]. For the same reason this method has its application in quantum information as well as in study of the entanglement in strongly interacting quantum systems [22, 23].

On the other hand, study of periodically driven many-body systems has regained interest after the recent experimental observation of drive induced delocalization phenomena [24]. The study of an equivalent non-interacting model reveals that such delocalization phenomena stems from the underlying chaotic dynamics [25]. In this context OTOC turns out to be an ideal method to explore the connection between the delocalization and the underlying chaos in an interacting quantum system. Although the connection of OTOC with Lyapunov exponent has been explored in several condensed matter systems [10–14], to the best of our knowledge the delocalization transition from many body localized (MBL) phases of quasiperiodic systems has not been investigated so far

using OTOC.

The experimental realization of quasiperiodic system such as the Aubry-André (AA) model has become a testbed to study single particle [26] as well as MBL phenomena of strongly interacting systems [27] since the AA model exhibits localization transition in 1D [28, 29]. In a recent experiment the dynamics of many body localized two component fermions subjected to a driven AA model reveals delocalization phenomena controlled by the frequency of the drive [24]. Motivated by this experiment, in this work we consider a system of strongly interacting bosons in the presence of an AA potential subjected to two different types of periodic drives which have different consequence on delocalization phenomena. Our goal is to study the commutator

$$C(\beta_T, p) = Tr \left[ \hat{\rho}_{\beta_T} [\hat{W}(p), \hat{V}(0)]^\dagger [\hat{W}(p), \hat{V}(0)] \right] \quad (1)$$

calculated after  $p^{\text{th}}$  drive cycle using the thermal density matrix  $\hat{\rho}_{\beta_T}$  at inverse temperature  $k_B\beta_T$  (where  $k_B$  is the Boltzmann constant), of suitable local unitary operators  $\hat{W}(p) \equiv \hat{W}(t = pT)$  and  $\hat{V}$  and to detect the delocalization transition in these driven systems from its behavior. We note that  $C(\beta_T, p)$  is related to the OTOC defined as

$$F(\beta_T, p) = Tr \left[ \hat{\rho}_{\beta_T} \hat{W}^\dagger(p) \hat{V}^\dagger(0) \hat{W}(p) \hat{V}(0) \right] \quad (2)$$

via  $C(\beta_T, p) = 2(1 - Re[F(\beta_T, p)])$ . The last relation holds for operators  $\hat{W}$  and  $\hat{V}$  that satisfy  $\hat{W}^2 = \hat{V}^2 = \hat{I}$ ; we shall always focus on such operators here.

Since in the semiclassical limit the Lyapunov exponent of the corresponding quantum system can be estimated from the unequal time commutator of conjugate dynamical variables [13], it is natural to expect that  $F(\beta_T, p)$  (and equivalently  $C(\beta_T, p)$ ) would capture thermalization and underlying chaos in a quantum many body system and thereby distinguish between its MBL and ergodic phases. In this work, by carrying out a detailed

study of properties of the OTOC for two periodically driven boson models in the presence of an Aubry-André (AA) potential, we show that this is indeed the case. We discuss the dependence of the OTOC on the time period  $T$  of the drive and show that both its saturation value and spectral properties can distinguish between MBL and ergodic phases; our results thus show that these quantities can serve as an indicator of delocalization transition even for systems with no obvious semiclassical or large  $N$  limit and thus with no clear definition of Lyapunov exponents.

We start by constructing the Floquet operator to generalize OTOC for stroboscopic dynamics and compare the behavior of  $C(\beta_T, p)$  with the spectral properties of the Floquet operator which has become a standard method to identify delocalization transition. The most general Hamiltonian describing a system under periodic perturbation is given by,

$$\hat{H}(t) = \hat{H}_0 + \hat{H}_1(t) \quad (3)$$

where  $\hat{H}_0$  is time independent part and the time dependent part satisfies  $\hat{H}_1(t+T) = \hat{H}_1(t)$ , where  $T$  is the time period of the drive. The corresponding Floquet operator is  $\hat{\mathcal{F}} = \hat{\mathcal{T}} e^{-i \int_0^T \hat{H}(t) dt / \hbar}$ , where  $\hat{\mathcal{T}}$  is the time ordering operator. Due to unitarity of  $\hat{\mathcal{F}}$ , the eigenvalue equation can be written as:  $\hat{\mathcal{F}}|\psi_\nu\rangle = e^{-i\phi_\nu}|\psi_\nu\rangle$ , where  $\phi_\nu$  and  $|\psi_\nu\rangle$  are the eigenphase and the eigenstate corresponding to the  $\nu$ th eigenmode of  $\hat{\mathcal{F}}$ . For periodically driven system the OTOC,  $F$  corresponding to two unitary operators  $\hat{W}$  and  $\hat{V}$  after the  $p^{\text{th}}$  drive cycle is given by Eq. 2 with  $\hat{W}(p) = \hat{\mathcal{F}}^{\dagger p} \hat{W}(0) \hat{\mathcal{F}}^p$ . In what follows, we shall describe two physical models and analyze the effect of the drive from the properties of Floquet operator and OTOC.

*Model I*: We consider a periodically driven system of hardcore bosons within tight binding approximation given by the Hamiltonian,

$$\hat{H}_0 = -J \sum_l (\hat{b}_l^\dagger \hat{b}_{l+1} + h.c.) + \mathcal{V} \sum_l \hat{n}_l \hat{n}_{l+1} \quad (4a)$$

$$\hat{H}_1(t) = \lambda (1 + \epsilon f(t)) \sum_l \cos(2\pi\beta l) \hat{n}_l, \quad (4b)$$

where  $\hat{b}_l^\dagger$  and  $\hat{n}_l = \hat{b}_l^\dagger \hat{b}_l$  are the creation and the density operators of the bosons at the  $l^{\text{th}}$  lattice site respectively,  $J$  is the hopping amplitude,  $\mathcal{V}$  is the strength of the nearest neighbor interaction,  $\lambda$  denotes the amplitude of the quasiperiodic potential, and  $\beta = (\sqrt{5} - 1)/2$ . For simplicity we consider a square pulse protocol in the interval  $x = 2\pi t/T \in [0, 2\pi]$  given by  $f(x) = \theta(x - \pi) - \theta(\pi - x)$ , where  $\theta(x)$  is the Heaviside step function. In rest of the paper, we set  $\hbar = 1$ , all energies (times) are measured in unit of  $J(1/J)$  and we consider  $\lambda = 3$  and  $\epsilon = 0.47$  such that the time independent Hamiltonian represents the localized regime of the AA model and drive induces mixing with the delocalized regime. All the plots shown

below are done for number of lattice sites  $N_s = 12$  at the half filling.

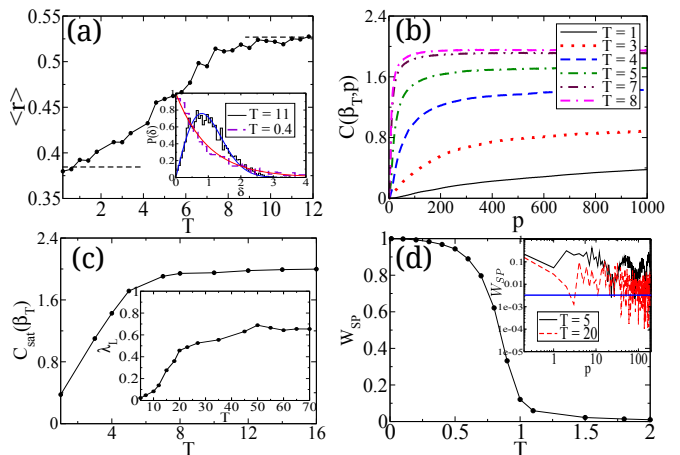


FIG. 1: (a)  $\langle r \rangle$  is shown as function of  $T$  and the spacing distribution of  $\delta_\nu$ 's for two typical values of  $T$  given in the inset; the corresponding probability distributions are shown in solid curves. (b)  $C(\beta_T, p)$  is plotted with number of drive  $p$  for different values of driving time period  $T$ . (c) Variation of  $C_{sat}(\beta_T)$  is shown as a function of  $T$ . In the inset, variation of the growth rate  $\lambda_L$  is depicted with  $T$ . (d) The survival probability  $W_{SP}$  in the steady state is plotted as function of  $T$ . The stroboscopic time evolution of  $W_{SP}$  is shown in the inset for different  $T$ . The horizontal line denotes the GOE value of  $W_{SP}$ . The other parameters for this plot are  $\lambda = 3$ ,  $\epsilon = 0.47$ ,  $\mathcal{V} = 0.1$  and  $\beta_T = 0.1$ .

We first find out the eigenphases,  $\phi_\nu$  of the corresponding Floquet operator and order them in  $[-\pi, \pi]$ . To quantify the degree of delocalization as well as to identify the change in the corresponding spectral statistics, we calculate the ratio between the consecutive level spacing,  $r_\nu = \min(\delta_{\nu+1}, \delta_\nu) / \max(\delta_{\nu+1}, \delta_\nu)$ , where  $\delta_\nu = \phi_{\nu+1} - \phi_\nu$ . We compute the average level spacing ratio  $\langle r \rangle$ , which, in the localized regime,  $\langle r \rangle \approx 0.386$  signifying that the normalized spacing distribution follows Poisson statistics, whereas in the delocalized regime  $\langle r \rangle \approx 0.527$  corresponds to the orthogonal class of RMT [30, 31]. From Fig. 1(a) we see that the value of  $\langle r \rangle$  gradually increases from 0.386 and reaches a value 0.527 with the increase in the time period indicating the thermalization induced by the periodic drive.

Next we investigate the time evolution of the commutator  $C(\beta_T, p)$  constructed from an equivalent local Pauli spin operators  $\hat{W}(\hat{V}) = \hat{\sigma}_z^l (\hat{\sigma}_z^l)$  where  $\hat{\sigma}_z^{l(l')}$  =  $2\hat{n}_{l(l')} - 1$ . We expect that in the MBL phase  $\hat{\sigma}_z^l$  commutes with the Hamiltonian due to the suppression of the kinetic energy resulting in a very slow growth of  $C(\beta_T, p)$ . On the other hand the kinetic energy term becomes significant which can give rise to non-trivial growth of  $C(\beta_T, p)$  in the delocalized regime. In Fig. 1(b) we have shown the stroboscopic time evolution of  $C(\beta_T, p)$  for different driving time period  $T$ . We observe that unlike the

large  $N$  models, in the delocalized regime the growth of  $C(\beta_T, p)$  is linear and there is no such scrambling phenomena observed in this driven system. This is apparently due to the fact that the driving time period is much larger compared to the typical scrambling time scale; therefore the stroboscopic time evolution cannot capture this phenomena. However,  $C(\beta_T, p)$  saturates eventually in the stroboscopic evolution; the saturation value  $C_{sat}(\beta_T) = \lim_{p \rightarrow \infty} C(\beta_T, p)$  increases with increasing driving time period  $T$  and finally for large  $T$  it saturates to the value  $C_{sat}(\beta_T) \sim 2$  as depicted in Fig. 1(c). The relation of the saturation value of  $C_{sat}(\beta_T)$  with that obtained using simple random matrix models is discussed in the supplementary material [32]. Further we fit the growth of  $C(\beta_T, p)$  with a function  $C_{sat}(\beta_T)(1 - e^{-p\lambda_L})$  where  $\lambda_L$  represents the growth rate and increases with increasing  $T$  as illustrated in the inset of Fig. 1(c). We note that both the behavior of  $C_{sat}(\beta_T)$  and  $\lambda_L$  resembles the behavior of  $\langle r \rangle$  and therefore can identify the delocalization crossover with the variation of driving time period  $T$ .

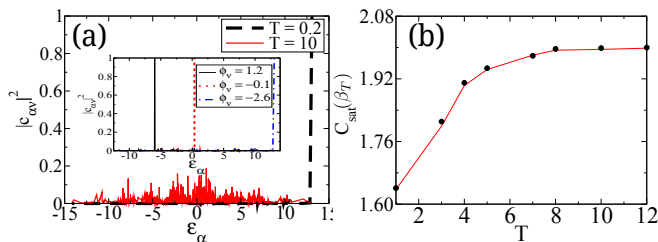


FIG. 2: (a) The overlap  $|c_{\alpha\nu}|^2$  is shown as a function of  $\epsilon_\alpha$  for a representative  $\phi_\nu$  corresponding to the lowest eigenmode of  $\hat{\mathcal{F}}$ . In the inset the same has been plotted for  $T = 0.2$  and the eigenmodes corresponding to lowest, middle and upper Floquet band. (b)  $C_{sat}(\beta_T)$  is shown as a function of  $T$  for  $l = l'$ . The solid line is obtained from Eq. 11 and the circles represent the values obtained from full stroboscopic time evolution. All other parameters are same as in Fig. 1.

The crossover to delocalized phase can also be captured from the survival probability [33] of an initially prepared state in the course of time evolution which is analogous to ‘imbalance factor’ measured in the experiments to capture the delocalization transition [27]. In the dynamical evolution we choose the initial state  $|\Psi(0)\rangle$  to be the ground state of the undriven Hamiltonian. During the stroboscopic time evolution in presence of drive the survival probability of the initial state can be computed from  $W_{SP}(p) = |\langle \Psi(0) | \hat{\mathcal{F}}^p | \Psi(0) \rangle|^2$ . In the MBL phase  $W_{SP}$  remains close to unity, whereas it decays in the delocalized regime. We compute the saturation value of  $W_{SP}$  in the steady state (obtained for  $p \simeq 1000$  in our numerics) and depict its variation as a function of  $T$  in Fig. 1(d). In well inside the delocalized regime  $W_{SP}$  saturates to  $\sim 3/D$  [see the inset in Fig. 1(d)] which is in

accordance with the RMT prediction [33],  $D$  being the dimension of the Hilbert space.

In order to understand the physics behind the decay of the survival probability, we calculate the overlap of the Floquet states with the eigenstates of the undriven Hamiltonian. We compute the quantity  $c_{\alpha\nu} = \langle \psi_\nu | v_\alpha \rangle$ , where  $|v_\alpha\rangle$  is the eigenstate corresponding to the  $\alpha$ th eigenmode of the undriven Hamiltonian. In Fig. 2(a) we have shown  $|c_{\alpha\nu}|^2$  corresponding to the Floquet state with eigenphase  $\phi_\nu$  as a function of the eigenenergies  $\epsilon_\alpha$  of the undriven Hamiltonian. We observe that in the small  $T$  regime typically the Floquet states have maximal overlap with one of the eigenstates of the undriven Hamiltonian indicating localization, whereas for higher  $T$  the overlap function  $|c_{\alpha\nu}|^2$  spreads over all the eigenmodes  $|v_\alpha\rangle$ . This observation allows us to consider that in the localized regime, the local operators  $\hat{\sigma}_z^l$  are diagonal in the Floquet basis. The saturation value of  $F$  with  $\hat{W} = \hat{V} = \hat{\sigma}_z^l$  is independent of  $l$  and can be approximated by [32],

$$F(\beta_T, p \rightarrow \infty) = \sum_{\alpha, \nu} \rho_{\beta_T}^\alpha |c_{\alpha\nu}|^2 s_{\nu\nu}^4 \quad (5)$$

where  $\rho_{\beta_T}^\alpha = e^{-\beta_T \epsilon_\alpha} / \sum_\alpha e^{-\beta_T \epsilon_\alpha}$  are elements of the initial thermal density matrix,  $c_{\alpha\nu} = \langle v_\alpha | \psi_\nu \rangle$  and  $s_{\nu\nu} = \langle \psi_\nu | \hat{\sigma}_z | \psi_\nu \rangle$ . This approximate analytical formula surprisingly agrees well with the results obtained from the full stroboscopic dynamics even for large  $T$  as illustrated in Fig. 2(b). From the above expression it can also be noted that in the delocalized regime the saturation value  $C_{sat}(\beta_T)$  becomes independent of the temperature scale due to the spreading of the overlap function  $|c_{\alpha\nu}|^2 \sim 1/D$  [see Fig. 2(a)] [32]. On the contrary in the localized regime (for smaller  $T$ ),  $C_{sat}(\beta_T)$  exhibits a strong temperature dependence and decreases with increasing  $\beta_T$ ; finally in the delocalized regime  $C_{sat}(\beta_T)$  attains the maximum value 2 signifying the infinite temperature thermalization in driven systems [34] as illustrated in [32]. Therefore this temperature dependence of the OTOC serve as a indicator of the degree of localization [15]

*Model II* : In the second case we consider a different type of drive applied to a system of strongly interacting bosons in a quasiperiodic potential which is described by the Hamiltonian

$$\begin{aligned} \hat{H}_0 &= \sum_l \left[ -J \left( \hat{b}_l^\dagger \hat{b}_{l+1} + h.c. \right) + \mathcal{V} \hat{n}_l \hat{n}_{l+1} \right] \quad (6) \\ &+ \lambda \cos(2\pi\beta l) \hat{n}_l, \quad \hat{H}_1(t) = 4\Delta f'(\omega t) / T \sum_l l \hat{n}_l \end{aligned}$$

where,  $\Delta$  is the driving amplitude and  $f'(x) = \theta(x - \pi/2) - 2\theta(x - 3\pi/2) - \theta(\pi/2 - x)$ . Such a drive gives rise to a nontrivial effect on the localization phenomena which has been explored in Ref. [25]. In the non-interacting limit of the above model, it has been shown that there

is a domain of frequency interval within which there appears a delocalized Floquet band which stems from the underlying chaotic dynamics of the equivalent classical model [25]. This is a counterintuitive scenario since such a drive in absence of quasiperiodic potential leads to the suppression of kinetic energy of the time averaged Hamiltonian [35, 36], hence expected to favor localization. To explore such phenomena and its connection with the underlying chaos in the interacting many body system we now follow the similar procedure as outlined in *Model I*.

First we analyze the Floquet spectrum  $\phi_\nu$  and compute the average level spacing ratio  $\langle r \rangle$  to characterize the delocalized as well as the localized phase. In Fig. 3(a) we have shown  $\langle r \rangle$  as a function of driving time period  $T$ . In the small  $T$  regime as well as for large  $T$ ,  $\langle r \rangle \sim 0.386$  indicating the localized Floquet states; the corresponding spacing distribution of the eigenphases exhibit Poisson distribution as shown in the inset of Fig. 3(a). On the other hand, in the intermediate regime  $\langle r \rangle$  increases with increasing  $T$  and shows a peak at  $T \sim 25$  exhibiting the level repulsion in the corresponding spacing distribution as depicted in the inset of Fig. 3(a). To further analyze this non-monotonic behavior of  $\langle r \rangle$ , we compute  $C_{sat}(\beta_T)$  and plotted it as a function of  $T$  in Fig. 3(b). We see that  $C_{sat}(\beta_T)$  shows a maximum at  $T \sim 25$  and decreases on both the side resembling the non-monotonic behavior of  $\langle r \rangle$ . Although the peak values of both the quantities  $\langle r \rangle$  and  $C_{sat}(\beta_T)$  are less than that of the GOE limit, but it clearly distinguishes from the MBL phase and indicates an approach to thermalization.

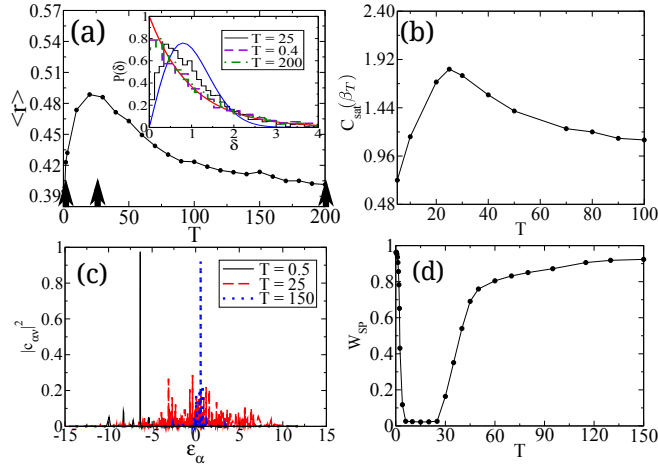


FIG. 3: (a) Variation of  $\langle r \rangle$  is shown as a function of  $T$ . In the inset the distribution of the spacing  $\delta_\nu$ 's are shown for three typical values of  $T$  mentioned therein; the corresponding probability distributions are shown by the solid lines.  $C_{sat}(\beta_T)$  and  $W_{SP}$  is plotted with increasing  $T$  in (b) and (d) respectively. (c) The overlap  $|c_{\alpha\nu}|^2$  is shown as a function of  $\epsilon_\alpha$  for a representative  $\phi_\nu$  corresponding to the lowest eigenmode of  $\hat{\mathcal{F}}$ . The other parameters are  $\lambda = 3$ ,  $\Delta = 1$ ,  $\mathcal{V} = 0.1$  and  $\beta_T = 0.1$ .

To explore the connection of underlying chaos with the

delocalization of the many body Floquet states, we compute the overlap function  $|c_{\alpha\nu}|^2$  and plotted it in Fig. 3(c) for different values of  $T$ . For small as well as for larger values of  $T$ ,  $|c_{\alpha\nu}|^2$  shows maximum overlap with one of the eigenmodes of the undriven Hamiltonian in Eq. 6 indicating localization, whereas, for intermediate values of  $T \sim 25$  the overlap function spreads over the eigenmodes  $|v_\alpha\rangle$  showing delocalization of the Floquet states. The peak in  $C_{sat}(\beta_T)$  and the spreading of the overlap function  $|c_{\alpha\nu}|^2$  indicates that such delocalization phenomena within an intermediate domain of  $T$  is a manifestation of the underlying chaos in the many body system. The delocalization of the Floquet states further results in the decay of survival probability  $W_{SP}$  around  $T \sim 25$ . In Fig. 3(d) we have shown the behavior of  $W_{SP}$  as a function of  $T$ ; the dip around  $T \sim 25$  indicates delocalization and the minimum value approaches the GOE limit. Such a domain of  $T$  where delocalized Floquet states appear can also be captured from the entanglement entropy and has been illustrated in Ref.[25].

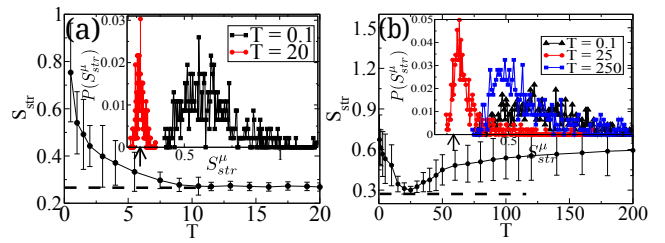


FIG. 4:  $\langle S_{str} \rangle$  is plotted with increasing  $T$  in (a) and (b) corresponding to *Model I* and *II* respectively. The error bars indicate the width  $\Delta S_{str}$  of the distribution of structural entropy  $P(S_{str}^\mu)$ , shown in the inset of both the figures for typical values of  $T$  mentioned therein. The horizontal dashed lines indicate the GUE value of the structural entropy.

*Statistics of OTOC* : Next, we focus on the statistics of OTOC motivated by a recent observation that the level spacing distribution of the OTOC corresponding to a single particle chaotic Hamiltonian exhibits a level repulsion analogous to the Gaussian unitary (GUE) universality class [14]. In what follows we test the statistics obtained from the eigenmodes of the OTOC operator  $\hat{F} = \hat{W}^\dagger(p)\hat{V}^\dagger(0)\hat{W}(p)\hat{V}(0)$  to distinguish the delocalization and thermalization phenomena in a driven many body system. We compute the operator,  $\hat{F}$  after sufficient number of drives and calculate the structural entropy  $S_{str}^\mu$  of the  $\mu$ th eigenmode  $|e_\mu\rangle$  of  $\hat{F}$ , defined as [37],

$$S_{str}^\mu = - \sum_{\chi} |c_\chi^\mu|^2 \ln |c_\chi^\mu|^2 - \ln \xi_\mu, \quad (7)$$

where  $c_\chi^\mu = \langle \chi | e_\mu \rangle$  is the overlap of  $|e_\mu\rangle$  with the computational basis  $|\chi\rangle$  and  $\xi_\mu = 1 / \sum_{\chi} |c_\chi^\mu|^4$  is the corresponding inverse participation ratio (IPR). For the eigenvectors

of the random matrices of Gaussian unitary class, the average structural entropy  $S_{str}$  approaches to a universal value  $\approx 0.27$  [38] independent of the dimensionality of the Hilbert space. In Fig. 4(a),(b) we have shown the variation of  $S_{str}$  with increasing  $T$  for both *Model I, II* respectively. The distribution of the structural entropy  $P(S_{str}^\mu)$  is shown in the inset for different values of  $T$  belonging to the localized regime and the delocalized regime. We notice that in the regime where thermalization occurs in both the models, structural entropy is sharply peaked at the value  $\sim 0.27$  indicating the GUE universality class. On the other hand in the localized regime, the peak vanishes and  $P(S_{str}^\mu)$  shows a broad distribution with increasing width  $\Delta S_{str} = \sqrt{\langle S_{str}^{\mu 2} \rangle - \langle S_{str}^\mu \rangle^2}$  shown by the error bars. This observation confirms that the statistics of OTOC can be an alternate method to detect the delocalization in a strongly interacting driven system.

*Conclusion :* To summarize we have studied the behavior of OTOC to detect the delocalization transition in a strongly interacting bosonic system in presence of a quasiperiodic potential subjected to two types of periodic drives showing distinctly different phenomena. We have shown that the saturation value  $C_{sat}(\beta_T)$ , the survival probability  $W_{SP}$ , and the spectral property of the OTOC can efficiently distinguish between the localized and the delocalized regime. Moreover recent experiments on the measurement of OTOC in trapped ion and NMR systems [18, 19] provide the way to calculate the saturation value  $C_{sat}(\beta_T)$  and can further be implemented to study such delocalization transition in a system of strongly interacting bosons in driven AA potential. The survival probability can be measured in experiment from the decay of an initially prepared state of the system in a similar way as has been done to measure the ‘imbalance factor’ in the cold atom experiments [24, 27]. It is a general belief that the growth of  $C(\beta_T, p)$  can capture the chaotic behavior of a quantum system. In previously studied non-interacting AA model under similar driving protocol it has been shown that the drive induced delocalization phenomena is connected with the chaotic dynamics of the corresponding classical model [25]. Our present study also confirms that the delocalization phenomena has a connection with the underlying chaotic dynamics of an interacting quantum system even when a direct classical correspondence is absent. Our results thus provide an alternate approach to diagnose the chaos as well as its connection with the thermalization in driven interacting many body systems and can be tested in the experiments in a similar line of thought as in [18, 19, 24, 27].

Stochastic behavior of a quantum pendulum under a periodic perturbation, in *Stochastic Behavior in Classical and Quantum Hamiltonian Systems*, G. Casati and J. Ford, eds., Lecture Notes in Physics, Vol. 93, Springer Berlin Heidelberg, 1979, pp. 334-352.

- [3] S. Chaudhury, A. Smith, B. E. Anderson, S. Ghose and P. S. Jessen, *Nature (London)* **461**, 768 (2009); C. Neill *et al.*, *Nat. Phys.* **12**, 1037 (2016).
- [4] A. M. Kaufman, M. E. Tai, A. Lukin, M. Rispoli, R. Schittko, P. M. Preiss and M. Greiner, *Science* **353**, 794 (2016).
- [5] J. M. Deutsch, *Phys. Rev. A* **43**, 2046 (1991); M. Srednicki, *Phys. Rev. E* **50**, 888 (1994).
- [6] F. Borgonovi, F.M. Izrailev, L. F. Santos, V. G. Zelevinsky, *Physics Reports* 626 (2016) 1-58; L D’Alessio, Y Kafri, A Polkovnikov, and M Rigol, *Adv. Phys.* **65**, 239 (2016).
- [7] O. Bohigas, M. J. Giannoni and C. Schmit, *Phys. Rev. Lett.* **52**, 1 (1984); O. Bohigas, M. J. Giannoni and C. Schmit, *J. Physique Lett.* **45**, 1015-1022 (1984).
- [8] A. Larkin and Y. N. Ovchinnikov, *JETP* **28**, 1200 (1969); D. A. Roberts and B. Swingle, *Phys. Rev. Lett.* **117**, 091602 (2016).
- [9] K. Hashimoto, K. Murata and R. Yoshii, *JHEP* **10**, 138 (2017).
- [10] B. Swingle and D. Chowdhury, *Phys. Rev. B* **95**, 060201(R) (2017); A. A. Patel, D. Chowdhury, S. Sachdev and B. Swingle, *Phys. Rev. X* **7**, 031047 (2017).
- [11] N. Y. Yao, F. Grusdt, B. Swingle, M. D. Lukin, D. M. Stamper-Kurn, J. E. Moore, E. Demler, arXiv:1607.01801 (2016).
- [12] A. Bohrdt, C. B. Mendl, M. Endres and M. Knap, *New J. Phys.* **19**, 063001 (2017).
- [13] E. B. Rozenbaum, S. Ganeshan and V. Galitski, *Phys. Rev. Lett.* **118**, 086801 (2017).
- [14] E. B. Rozenbaum, S. Ganeshan and V. Galitski, arXiv:1801.10591 (2018).
- [15] X. Chen, T. Zhou, D. A. Huse and E. Fradkin, *Ann. Phys. (Berlin)* **529**, 1600332 (2017).
- [16] M. Heyl, F. Pollmann and B. Dóra, arXiv:1801.01684 (2018); A. Das, S. Chakrabarty, A. Dhar, A. Kundu, R. Moessner, S. S. Ray, and S. Bhattacharjee, arXiv:1711.07505 (2017); C. Lin and O. I. Motrunich, arXiv:1801.01636 (2018).
- [17] P. Bordia, F. Alet and P. Hosur, *Phys. Rev. A* **97**, 030103(R) (2018); G. Zhu, M. Hafezi and T. Grover, *Phys. Rev. A* **94**, 062329 (2016).
- [18] M. Gärttner, J. G. Bohnet, A. Safavi-Naini, M. L. Wall, J. J. Bollinger and A. M. Rey, *Nature Physics* **13**, 781-786 (2017).
- [19] J. Li, R. Fan, H. Wang, B. Ye, B. Zeng, H. Zhai, X. Peng and J. Du, *Phys. Rev. X* **7**, 031011 (2017).
- [20] S. Sachdev and J. Ye, *Phys. Rev. Lett.* **70**, 3339 (1993); A. Kitaev, *Hidden correlations in the Hawking radiation and thermal noise*, in Talk given at the Fundamental Physics Prize Symposium, Vol. 10 (2014).
- [21] S. H. Shenker and D. Stanford, *JHEP* **03**, 067 (2014); J. Maldacena, S. H. Shenker, and D. Stanford, *JHEP* **08**, 106 (2016)
- [22] M. Gärttner, P. Hauke and A. Rey, *Phys. Rev. Lett.* **120**, 040402 (2018); P. Hosur, X.-L. Qi, D. A. Roberts, B. Yoshida, *JHEP* **2**, 4 (2016); R. Fan, P. Zhang, H. Shen, H. Zhai, *Science Bulletin* **62**, 707 (2017).
- [23] B. Swingle, G. Bentsen, M. Schleier-Smith and P. Hay-

---

[1] Fritz Haake, *Quantum signatures of chaos*, Vol. 54. Springer Science and Business Media, 2013.  
 [2] G. Casati, B. V. Chirikov, F. M. Izrailev, and J. Ford,

- den, Phys. Rev. A **94**, 040302(R) (2016)
- [24] P. Bordia, H. Lüschen, U. Schneider, M. Knap and I. Bloch, *Nat. Phys.* **13**, 460 (2017).
- [25] S. Ray, A. Ghosh and S. Sinha, Phys. Rev. E **97**, 010101(R) (2018).
- [26] G. Roati *et al.*, Nature (London) **453**, 895 (2008).
- [27] M. Schreiber *et al.*, Science **349**, 842 (2015); J.-y. Choi *et al.*, Science **352**, 1547 (2016); P. Bordia, H. P. Lüschen, S. S. Hodgman, M. Schreiber, I. Bloch and U. Schneider, Phys. Rev. Lett. **116**, 140401 (2016); P. Bordia, H. Lüschen, S. Scherg, S. Gopalakrishnan, M. Knap, U. Schneider and I. Bloch, arXiv:1704.03063 (2017); H. P. Lschen, P. Bordia, S. Scherg, F. Alet, E. Altman, U. Schneider and I. Bloch, Phys. Rev. Lett. **119**, 260401 (2017).
- [28] S. Aubry and G. André, Ann. Isr. Phys. Soc. **3**, 133 (1980).
- [29] C. Aulbach, A. Wobst, G. L. Ingold, P. Hänggi, and I. Varga, New J. Phys. **6**, 70 (2004).
- [30] V. Oganesyan and D. A. Huse, Phys. Rev. B **75**, 155111 (2007); S. Iyer, V. Oganesyan, G. Refael and D. A. Huse, Phys. Rev. B **87**, 134202 (2013).
- [31] Y. Y. Atas, E. Bogomolny, O. Giraud, and G. Roux, Phys. Rev. Lett. **110**, 084101 (2013).
- [32] See supplementary materials for more details.
- [33] E. J. Torres-Herrera, A. M. García-García and L. F. Santos, Phys. Rev. B **97**, 060303(R) (2018); E. J. Torres-Herrera, J. Karp, M. Távora, L. F. Santos, Entropy **18**, 359 (2016); S. Lerma-Hernández, J. Chávez-Carlos, M. A. Bastarrachea-Magnani, L. F. Santos, J. G. Hirsch, arXiv:1710.05937 (2017); L. F. Santos and E. J. Torres-Herrera, arXiv:1803.06012 (2018).
- [34] L. DAlessio and M. Rigol, Phys. Rev. X **4**, 041048 (2014); H. Kim, T. N. Ikeda and D. A. Huse, Phys. Rev. E **90**, 052105 (2014); S. Ray, A. Ghosh and S. Sinha, Phys. Rev. E **94**, 032103 (2016); A. Russomanno, R. Fazio and G. E. Santoro, *Europhysics Letters* **110**, 37005 (2015); N. Regnault and R. Nandkishore, Phys. Rev. B **93**, 104203 (2016).
- [35] A. Eckardt, Rev. Mod. Phys. **89**, 011004 (2017).
- [36] H. Lignier, C. Sias, D. Ciampini, Y. Singh, A. Zenesini, O. Morsch and E. Arimondo, Phys. Rev. Lett. **99**, 220403 (2007); C. Sias, H. Lignier, Y. P. Singh, A. Zenesini, D. Ciampini, O. Morsch and E. Arimondo, Phys. Rev. Lett. **100**, 040404 (2008); A. Eckardt, M. Holthaus, H. Lignier, A. Zenesini, D. Ciampini, O. Morsch and E. Arimondo, Phys. Rev. A **79**, 013611 (2009).
- [37] János Pipek and Imre Varga, Phys. Rev. A **46**, 3148 (1992); P. Jacquod and I. Varga, Phys. Rev. Lett. **89**, 134101 (2002).
- [38] F. M. Izrailev, Phys. Rep. **196**, 299 (1990); *ibid.* **276**, 85 (1996); S. Ray, B. Mukherjee, S. Sinha and K. Sengupta, Phys. Rev. A **96**, 023607 (2017).

## SUPPLEMENTAL MATERIAL

In this supplemental material we provide the results of the full quantum dynamics governed by a model Hamiltonian consisting of a mixture of random matrix of Gaussian Orthogonal class (GOE) and a Poisson matrix. We also discuss the stroboscopic time evolution of the out-of-time-order correlator (OTOC) as well as discuss the temperature dependence of its saturation value.

### Evolution under GOE matrix

First, we consider the Hamiltonian describing a mixed random matrix ensemble given by,

$$\hat{H}_R = \hat{H}_P + \lambda \hat{H}_G / \sqrt{\mathcal{D}} \quad (8)$$

where  $\hat{H}_P$  is a random banded matrix exhibiting Poisson level spacing distribution,  $\hat{H}_G$  is a GOE matrix and  $\mathcal{D}$  is the size of the matrix. In what follows we construct the Floquet operator  $\hat{\mathcal{F}} = e^{-i\hat{H}_R T}$  and study its spectral properties as well as the dynamics governed by  $\hat{\mathcal{F}}$ . We note that here  $\lambda$  is a tuning parameter and in the limit  $\lambda \rightarrow 0$ ,  $\hat{H}_R$  is a Poisson matrix where as for  $\lambda \gg 1$ ,  $\hat{H}_R$  resembles a GOE matrix.

*Spectral Statistics* : From the eigenvalue equation  $\hat{\mathcal{F}}|\psi_\nu\rangle = e^{-i\phi_\nu}|\psi_\nu\rangle$ , we first compute the eigenphases  $\phi_\nu$  corresponding to the eigenmode  $|\psi_\nu\rangle$ . We compute the average level spacing ratio  $\langle r \rangle$  as defined in the main text and plotted it as a function of  $\lambda$  in Fig. 5(a). For small  $\lambda$ ,  $\langle r \rangle \sim 0.386$  indicating the Poisson distribution; further increase in  $\lambda$  results in an increase in  $\langle r \rangle$  and finally saturates to  $\sim 0.527$  representing the GOE class of the corresponding spacing distribution as depicted in Fig. 5(a).

*OTO Correlator* : To study the time evolution under  $\hat{\mathcal{F}}$ , we first construct the initial thermal density matrix as  $\hat{\rho}_{\beta_T} = e^{-\beta_T \hat{H}_P}$  so as to start from a localized system and evolve it stroboscopically. We calculate the commutator  $C(\beta_T, p)$  and plotted it as a function of  $p$  for different values of  $\lambda$  in Fig. 5(b). It can be noted that the growth rate of  $C(\beta_T, p)$  as well as the saturation value  $C_{sat}(\beta_T)$  obtained after sufficient number of drives increase with increasing  $\lambda$ . This is further illustrated in Fig. 5(c) where we have shown  $C_{sat}(\beta_T)$  as a function of  $\lambda$ . It is important to note that in the GOE regime  $F(\beta_T, p)$  decays very fast and becomes vanishingly small leading to  $C_{sat}(\beta_T) \sim 2$  as depicted in Fig. 5(c).



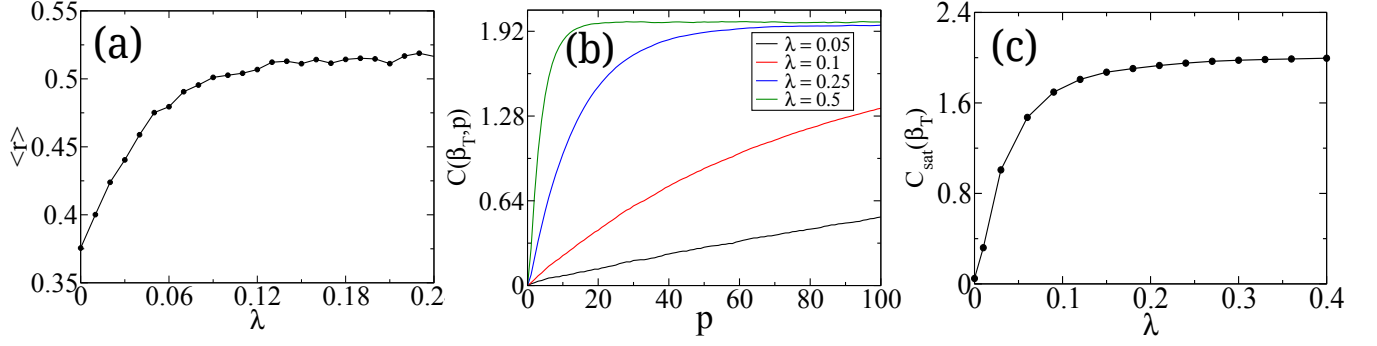


FIG. 5: (a)  $\langle r \rangle$  as a function of  $\lambda$ . (b) Stroboscopic time evolution of  $C(\beta_T, p)$  for different values of  $\lambda$ . (c) Saturation value  $C_{sat}(\beta_T)$  is plotted as a function of  $\lambda$ .

### Stroboscopic time evolution of OTOC for *Model I*

In this section we will study the stroboscopic evolution of the OTOC corresponding to *Model I* and also study its dependence on different system sizes in both the MBL phase and in the regime where thermalization occurs. To this end, we first sketch the derivation of Eq.(5) of the main text. The quantity  $F(\beta_T, p)$  after  $p$  cycles of the drive and at the inverse temperature  $\beta_T$  is given by

$$\begin{aligned} F(\beta_T, p) &= \text{Tr}[\hat{\rho}_{\beta_T} \hat{W}(p) \hat{V}(0) \hat{W}(p) \hat{V}(0)] \\ &= \sum_{\alpha} e^{-\beta_T \epsilon_{\alpha}} \langle v_{\alpha} | \hat{\mathcal{F}}^{\dagger} \hat{W}(0) \hat{\mathcal{F}} \hat{V}(0) \hat{\mathcal{F}}^{\dagger} \hat{W}(0) \hat{\mathcal{F}} \hat{V}(0) | v_{\alpha} \rangle / Z \end{aligned} \quad (9)$$

where  $\hat{\mathcal{F}}$  is the evolution operator and  $|v_{\alpha}\rangle$ ,  $\epsilon_{\alpha}$  denotes eigenvectors and eigenvalues of  $\hat{H}(t=0)$  (see Eq. 4 in the main text) and  $Z = \sum_{\alpha} \exp(-\beta_T \epsilon_{\alpha})$  is the corresponding partition function. We then decompose  $F$  in terms of its eigenstates  $|\psi_{\nu}\rangle$  and eigenenergies  $\phi_{\nu}$  (as defined in the main text). A few lines of algebra yields

$$F(\beta_T, p) = \frac{1}{Z} \sum_{\alpha} \sum_{\mu, \nu, \lambda, \mu', \nu'} c_{\alpha\mu}^* c_{\nu\alpha} e^{i(\phi_{\mu} + \phi_{\lambda} - \phi_{\mu'} - \phi_{\nu'}) p T} W_{\mu\mu'}(0) W_{\lambda\nu'}(0) V_{\mu'\lambda}(0) V_{\nu'\nu}(0). \quad (10)$$

Here  $c_{\alpha\nu} = \langle v_{\alpha} | \psi_{\nu} \rangle$  denotes the overlap function,  $T$  is the drive time period, and  $\mathcal{F}$  and  $W_{\nu\nu'}(0)$  denotes the matrix element of  $\hat{W}$  between Floquet eigenstates  $|\psi_{\nu}\rangle$  and  $|\psi_{\nu'}\rangle$ . For  $p \rightarrow \infty$ , the contribution to  $F$  is obtained from terms for which  $\phi_{\mu} + \phi_{\lambda} = \phi_{\mu'} + \phi_{\nu'}$ . Furthermore, numerically, we find that for  $\hat{W} = \hat{V} = \hat{\sigma}_z$ , these matrix elements have maximal contribution from the diagonal terms. Denoting  $\langle \psi_{\nu} | \hat{\sigma}_z | \psi_{\nu'} \rangle \simeq s_{\nu\nu'} \delta_{\nu\nu'}$ , we finally obtain,

$$F(\beta_T, p \rightarrow \infty) = \frac{\sum_{\alpha, \nu} e^{-\beta_T \epsilon_{\alpha}} |c_{\alpha\nu}|^2 s_{\nu\nu}^4}{\sum_{\alpha} e^{-\beta_T \epsilon_{\alpha}}} \quad (11)$$

which is Eq. (5) of the main text. We find that in the delocalized regime  $|c_{\alpha\nu}|^2 \sim 1/\mathcal{D}$  where  $\mathcal{D}$  is the dimension of the matrix. This results in the saturation value of  $C_{sat}(\beta_T) \sim 2$  indicating that such a driven system thermalizes to infinite temperature where  $C_{sat}(\beta_T)$  becomes independent of  $\beta_T$ .

In Fig. 1(a) of the main text it has been shown that the growth rate of  $C(\beta_T, p)$  is very small in the MBL phase, on the other hand  $C(\beta_T, p)$  grows very fast in the delocalized regime. In contrast the OTOC,  $F(\beta_T, p)$  shows a very slow power law decay in the MBL phase as depicted in a logarithmic plot in Fig. 6(b) and shows a very strong system size dependence in the saturation value. On the other hand, for large driving time period  $T$  OTOC decays exponentially fast and saturates to a vanishingly small value as shown in Fig. 6(c).

*Temperature dependence* : Further we study the temperature dependence of the OTOC. First we note that for large  $T$  when the system thermalizes, there is no such temperature dependence and  $F(\beta_T, p)$  decays exponentially resulting in the saturation value  $C_{sat}(\beta_T) \sim 2$ . Whereas for small  $T$  i.e. in the MBL phase, the saturation value of the OTOC increases with decreasing temperature resulting in the decrease in  $C_{sat}(\beta_T)$  with increasing  $\beta_T$  as illustrated in Fig. 6(a). Such a growth of OTOC can be understood as follows. We first note that in Eq. 11,  $\sum_{\nu} |c_{\alpha\nu}|^2 = 1$  for all  $\alpha$ ; moreover, it can be checked numerically  $s_{\nu\nu}^4 < 1$  for all  $\nu$ . Thus the quantity  $\mathcal{L}_{\alpha} = \sum_{\nu} |c_{\alpha\nu}|^2 s_{\nu\nu}^4 < 1$ , which ensures

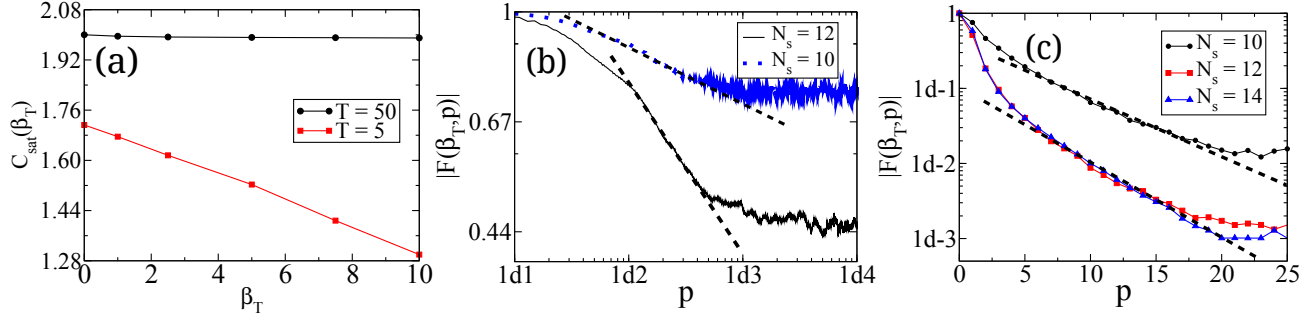


FIG. 6: (a)  $C_{sat}(\beta_T)$  is shown as a function of  $\beta_T$ . The stroboscopic time evolution of  $|F(\beta_T, p)|$  is shown in the localized regime for  $T = 5$  in (b) and in the delocalized regime for  $T = 50$  in (c). The dashed lines in (b) and (c) indicate the linear behavior in log-log plot and in semi-log plot respectively.

the convergence of the numerator of Eq. 11 since  $\epsilon_\alpha$  can always be chosen to be positive without any loss of generality. In terms of  $\mathcal{L}_\alpha$ , one can write

$$F(\beta_T, p \rightarrow \infty) = \frac{\sum_\alpha e^{-\beta_T \epsilon_\alpha} \mathcal{L}_\alpha}{\sum_\alpha e^{-\beta_T \epsilon_\alpha}} = \frac{N}{Z} \quad (12)$$

Using this expression, it is straightforward to see, that

$$\frac{\partial F(\beta_T, p \rightarrow \infty)}{\partial \beta_T} = \frac{1}{Z^2} \sum_{\alpha \neq \alpha'} e^{-\beta_T (\epsilon_\alpha + \epsilon_{\alpha'})} \epsilon_\alpha \mathcal{L}_{\alpha'} > 0 \quad (13)$$

Thus  $F(\beta_T, p \rightarrow \infty)$  must increase with increasing  $\beta_T$  leading to decrease of  $C_{sat}(\beta_T)$  with  $\beta_T$  as shown in Fig. 6(a).